The thermal decomposition of the new energetic material ammoniumdinitramide ($NH_4N(NO_2)_2$) in relation to Nitramide (NH_2NO_2) and NH_4NO_3

ARTICLE *in* INTERNATIONAL JOURNAL OF CHEMICAL KINETICS · JULY 1993

Impact Factor: 1.52 · DOI: 10.1002/kin.550250705

3 AUTHORS, INCLUDING:

Michel J Rossi
Paul Scherrer Institut
259 PUBLICATIONS **6,478** CITATIONS

The Thermal Decomposition of the New Energetic Material Ammoniumdinitramide ($NH_4N(NO_2)_2$) in Relation to Nitramide (NH_2NO_2) and NH_4NO_3

MICHEL J. ROSSI,* JEFFREY C. BOTTARO, and DONALD F. McMILLEN
Chemistry Laboratory, SRI International, Menlo Park, California 94025

Abstract

This qualitative study examines the response of the novel energetic material ammonium dinitramide (ADN), $NH_4N(NO_2)_2$, to thermal stress under low heating rate conditions in a new experimental apparatus. It involved a combination of residual gas mass spectrometry and FTIR absorption spectroscopy of a thin cryogenic condensate film resulting from deposition of ADN pyrolysis products on a KCl window. The results of ADN pyrolysis were compared under similar conditions with the behavior of NH_4NO_3 and NH_2NO_2 (nitramide), which served as reference materials. NH_4NO_3 decomposes into HNO_3 and NH_3 at 182°C and is regenerated on the cold cryostat surface. HNO_3 undergoes presumably heterogeneous loss to a minor extent such that the condensed film of NH_4NO_3 contains occluded NH_3. Nitramide undergoes efficient heterogeneous decomposition to N_2O and H_2O even at ambient temperature so that pyrolysis experiments at higher temperatures were not possible. However, the presence of nitramide can be monitored by mass spectrometry at its molecular ion (*m/e* 62). ADN pyrolysis is dominated by decomposition into NH_3 and $HN(NO_2)_2$ (HDN) in analogy to NH_4NO_3, with a maximum rate of decomposition under our conditions at approximately 155°C. The two vapor phase components regenerate ADN on the cold cryostat surface in addition to deposition of the pure acid HDN and H_2O. Condensed phase HDN is found to be stable for indefinite periods of time at ambient temperature and vacuum conditions, whereas fast heterogeneous decomposition of HDN at higher temperature leads to N_2O and HNO_3. The HNO_3 then undergoes fast (heterogeneous) decomposition in some experiments. Gas phase HDN also undergoes fast heterogeneous decomposition to NO and other products, probably on the internal surface (ca. 60°C) of the vacuum chamber before mass spectrometric detection.

Introduction

Nitramines are a familiar class of energetic compounds that are used either pure or in conjunction with other ingredients as propellants or explosives. On the other hand, previous preparations of dinitramines have been very limited and have produced only highly unstable materials of no practical use. Hamel and Olsen describe [1], in detail, the synthesis of alkyl N,N dinitramines from alkyl nitramines and nitronium fluoborate. These alkyl dinitramines are unstable, decomposing at temperatures of 75°C or less.

* To whom correspondence should be addressed at Ecole Polytechnique Fédérale de Lausanne, DGR/Laboratoire de Pollution Atmosphérique, Bâtiment CH/LCT, CH-1015 Lausanne, Switzerland.

International Journal of Chemical Kinetics, Vol. 25, 549–570 (1993)
 CCC 0538-8066/93/070549-22

The unfortunate thermal instability of these materials renders them useless as explosives, propellants, or propellant ingredients. However, the parent dinitramine (or "dinitraminic acid"), $HN(NO_2)_2$, as well as its salts, which were not previously known, display properties vastly different from those of alkyldinitramines. Recently, Bottaro and Schmitt have synthesized a series of salts of dinitramide that have been shown to be promising candidates for halogen-free efficient propellants. [2] The present study provides a qualitative assessment of the properties of the ammonium salt of dinitramide (ADN) under thermal stress in order to gain insight into the modes of thermal decomposition that could be of importance in the explosive decomposition of those materials. It is apparent from our results that experiments at higher heating rates have to be undertaken in order to understand, and hence model, the actual combustion or explosive decomposition of ADN or similar materials. However, our experiments allow us to catch a first glimpse on the possible reaction pathways and reaction products of those novel energetic materials.

We have also examined, under similar experimental conditions, two closely related nitrogen compounds as reference materials, namely NH_4NO_3 and NH_2NO_2, whose thermal decomposition have been studied in some detail previously. Although bulk kinetic studies of NH_4NO_3 have been performed by several authors [3–5], important mechanistic questions remain unanswered, even for this compound. We hope to learn more of the modes of rapid decomposition of the novel energetic materials by comparing their thermal behavior with these "reference" materials.

Experimental Apparatus and Approach

The apparatus used for this work was constructed to study the decomposition of organic materials by utilizing concurrent mass spectrometeric detection of vapor phase species and FTIR detection of condensible products. Since the decomposition of energetic materials is often characterized by multiple decomposition pathways and fast secondary reactions, heating at low pressures can provide a way to slow down the secondary reactions and facilitate observation of the initial decomposition steps. Since the branching ratios of the competing secondary reactions will likely change markedly with shifts in phase, concentration, and temperature, we expect low pressure studies by themselves to be insufficient to provide a practical understanding of the behavior of energetic materials. On the other hand, the behavior of these materials is typically so complex that examination under the nominal conditions of propellant combustion, for instance, will seldom, if ever, be sufficient to provide a real understanding of the chemistry that controls the combustion kinetics. Therefore, we have used the experimental apparatus shown schematically in Figure 1 to study and compare the low pressure condensed phase decomposition behavior of NH_4 NO_3, NH_2NO_2, and $NH_4(NO_2)_2$.

The strategy adopted is the following: About 1 mg is heated in a small pyrex capillary housed in a heated direct insertion probe that is located about 5 cm in front of a cryogenically cooled KCl window. The gaseous pyrolysis products hit a cryogenic (liquid N_2 cooled) window whose transmission in

the IR is examined at given time intervals by FTIR absorption spectroscopy, at the same time that the gas phase is sampled with a quadrupole mass spectrometer. Due to the fact that the thermal decomposition is taking place at nominal pressures of 10^{-7} torr, only the gaseous components with an equilibrium vapor pressure smaller than the background pressure will be deposited as an amorphous film onto the cryogenic window. Pyrolysis products that do not satisfy this condition will be monitored by mass spectrometry, which is performed in a residual gas mode in this series of experiments. Therefore, such products as N_2, NO, and N_2O have been monitored at m/e 28, 30, and 44, essentially in situ. The sensitivity of the FTIR absorption measurements is excellent because of the effective integration of the product flux by letting sufficient material accumulate onto the window, and also because of the high signal-to-noise ratios of the FTIR spectrophotometer. Once the sample has decomposed and the growth of the condensed phase on the IR optical window has ceased, the temperature of the cryostat is slowly increased. Thermal desorption of pyrolysis products monitored by mass spectrometry as the temperature of the cryostat is rising gives further insight into the nature and identity of the complex mixture of pyrolysis products.

The main cylindrical stainless steel vacuum chamber housing the cryostat (Fig. 1) is pumped by a 2000 $l\ s^{-1}$ baffled diffusion pump whose base pressure was 10^{-8} torr. In view of the low vapor pressure of many of the materials investigated in this and other studies, the walls of the vacuum chamber were heated to about 60°C in order to minimize "memory effects" of the samples studied. This heating resulted in a final temperature of the cryogenic KCl window (liquid N_2 cooled) of approximately −185 or −180°C, slightly higher than the temperature achieved without heating the chamber walls. Two total pressure ion gauges measure the pressure in the main vacuum chamber at two different locations. One is mounted near the top of the chamber near the cryostat, the second is located in proximity of the inlet to the 8″ diffusion pump. The mass spectrometry chamber is pumped by a 270 $l\ s^{-1}$ turbomolecular pump and houses a BALZERS QMG 511 quadrupole mass spectrometer operated in residual gas analysis mode. The mass spectrometer chamber can be isolated from the main deposition/pyrolysis vacuum chamber by a 6″ gate valve in case the pressure becomes too high in the mass spectral analysis chamber.

The heatable sample probe is shown in some more detail in Figure 2 and is designed to be inserted through a 0.5″ diameter aperture ball valve. The quartz probe can be completely retracted into the stainless steel sleeve during insertion or removal through the ball valve. The heating of the sample is performed by radiative transfer of energy from the heating wire to the sample across the quartz tubing. Note that the type "K" thermocouple is housed in a well beneath the sample and is separated from the NiCr heating wire by an amount of material (glass) comparable to that which separates the sample (contained in a thin walled pyrex melting capillary tube) from the heating wire.

The material requirements for pyrolysis are minimal in that 0.5 to 2 mg of solid material are placed in the bottom of 1-cm long melting point capillary which is then inserted into the probe tip. This amount is sufficient to obtain

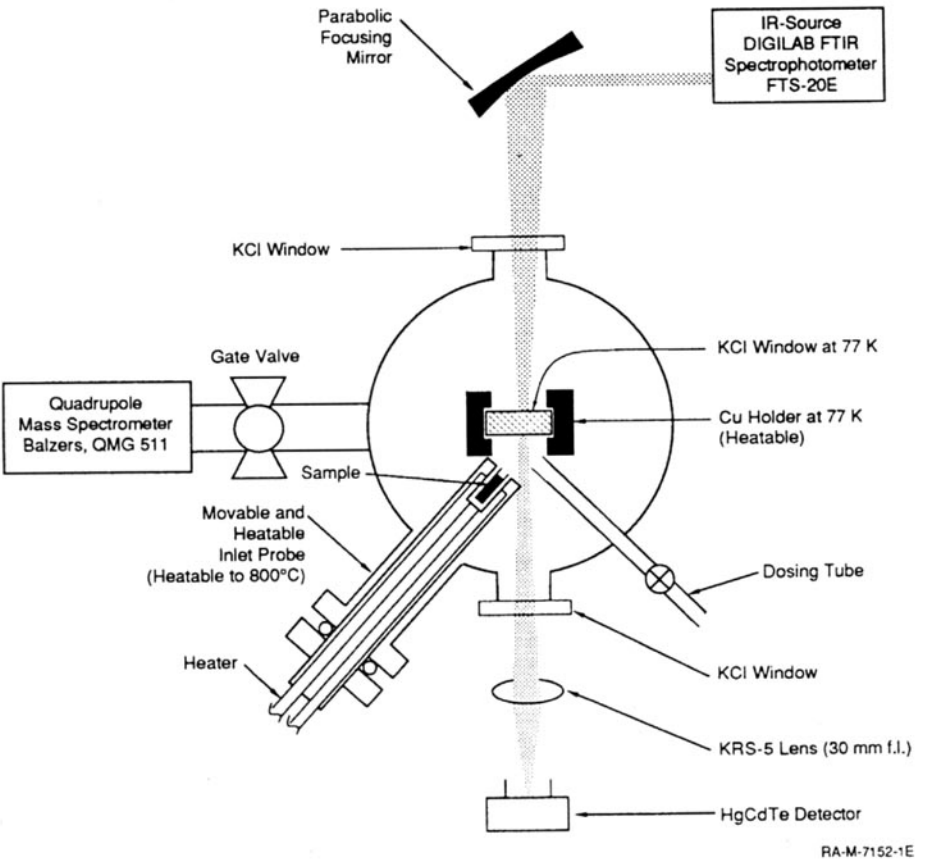

Figure 1. Thin film diagnostic apparatus using FTIR-absorption and mass spectrometry.

intense mass spectra and FTIR spectra of deposited thin films of μm size thickness, resulting in absorption spectra of excellent signal-to-noise ratio (≥ 100). Typically, the experimental protocol consists of increasing the probe temperature while collecting the pyrolysate on either the cold or ambient temperature KCl window, whose temperature is measured at the distant tip (furthest from the liquid N_2) using a type "*E*" thermocouple fastened with a screw to the copper frame of the 1″ diameter KCl IR transmission window. Once the material in the probe capillary is exhausted and has been collected on the KCl window, the latter is heated in order to desorb the condensate until the original IR transmission of the KCl window has been restored.

The cryostat is a 0.5″ diameter stainless steel tube holding liquid nitrogen. The upper portion of the cryostat is surrounded by a vacuum insulated concentric tube in order to ensure ambient temperature at the seal (knife-edge) to the top of the vacuum chamber. The tip of the cryostat is a brazed copper plug to which the copper window holder is fastened. For heating, the cryostat is wrapped on its entire length by a resistive heating element (ARI heaters) clamped to the cryostat by steel clamps. In some experiments temperatures of 300°C had to be attained in order to rid the KCl window of

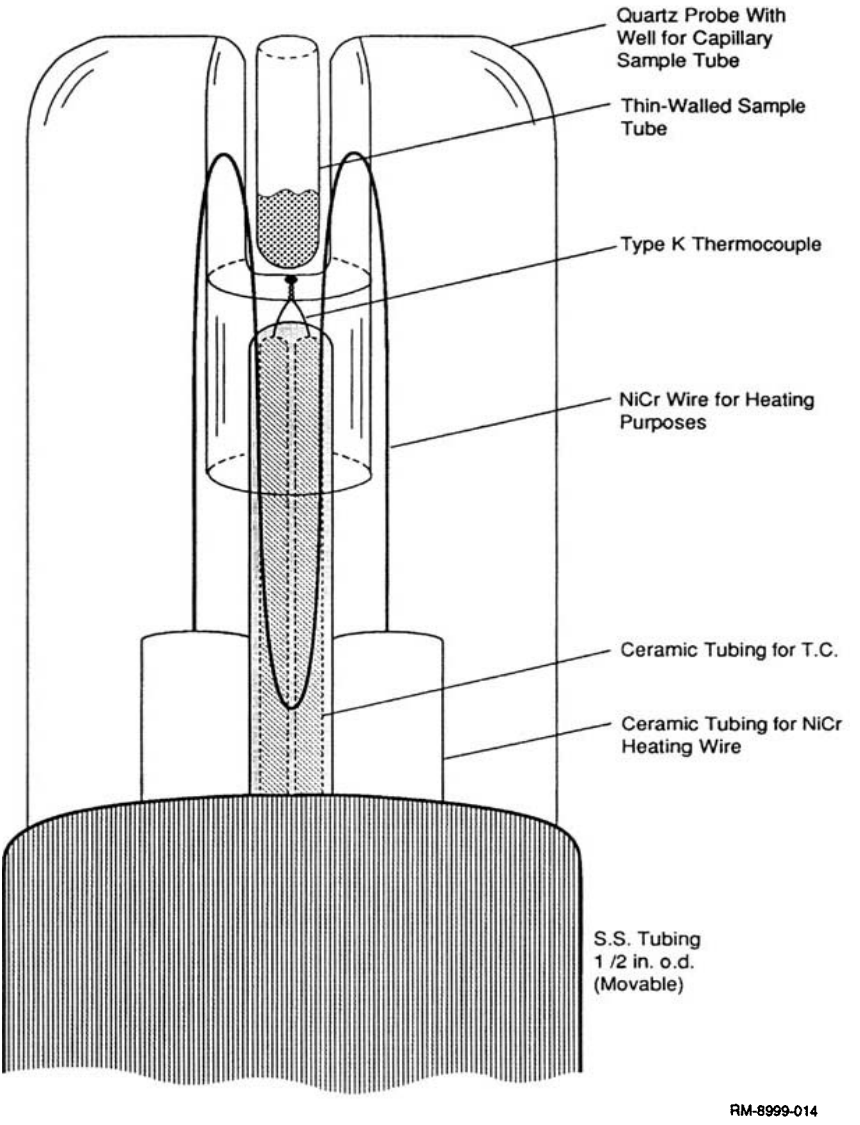

Figure 2. Schematic cross section of the resistively heated fused silica probe tip for holding capillary sample tubes.

any absorptions in the IR. In this way mass spectra for all the components of the pyrolysate are obtained as a function of temperature, whereas FTIR transmission spectra are obtained for those components that are collected onto the cryogenic window and that are stable with respect to evaporation and/or pyrolysis at a given probe temperature.

FTIR spectra are recorded using a DIGILAB FTS-20E spectrometer, whose external beam was not purged. Therefore, the resulting IR spectra show some presence of atmospheric constituents (CO_2, H_2O), even after spectral subtraction. IR radiation leaving the optics bench of the FTS-20E spectrometer was directed using two flat first surface Al mirrors onto a 3″ diameter first surface Al focussing mirror (f.l. 5″). The vacuum system was

sealed by two 2″ flat KCl windows. After passage through the cryogenic window at the tip of the cryostat, the beam was refocussed onto the wide-band HgCdTe detector (5000–500 cm^{-1}) using a 1″ diameter 1″ f.l. KRS-5 lens. In some experiments not detailed here, the thickness of the deposited amorphous film was measured using the interference fringes of a HeNe laser using the same focussing mirror as the IR beam (This is not shown in Fig. 1).

Nitramide, NH_2NO_2, and ammoniumdinitramide (ADN), $NH_4N(NO_2)_2$ were synthesized by Bottaro of SRI's Chemistry Laboratory [2]. The ammoniumdinitramide appeared to have a purity > 99%, with the only significant impurity (apart from water) being evidenced by small contributions at *m/e* 55 and 57, which originate from a small impurity of *n*–butanol which was used to recrystallize $NH_4N(NO_2)_2$.

Results and Discussion

In this article only qualitative results on the thermal decomposition of ammonium dinitramide will be presented. In order to put these results into the proper context, we will compare the behavior of ADN with that of NH_4NO_3 and NH_2NO_2 under thermal stress. The reason for this procedure is the fact that both NH_4NO_3 and NH_2NO_2 are possible intermediates of the thermal decomposition of $NH_4N(NO_2)_2$, although the connection is more formal than structural. We will present results on the two simpler nitrogen containing compounds prior to the discussion of ADN thermal decomposition. Throughout the discussion, we will usually refer to ammonium dinitramide by the acronym ADN, and for consistency to the free dinitraminic acid as HDN, although in deference to common usage, we will continue to use the name nitramide for NH_2NO_2.

NH_4NO_3

Quantities on the order of a milligram of ground NH_4NO_3 were placed in the probe with the cryogenic window at −190°C (83 K). Upon heating the probe, the effusing gases were monitored by mass spectrometry. Mass spectral scans revealed the presence of NH_3 and HNO_3 in increasing amounts with increasing probe temperature. NH_3 was monitored at masses *m/e* 16 and 17, whereas HNO_3 was followed at *m/e* 63, 46, and 30. Quantitative evaluation established these two gas phase products as the only vapor phase species of importance. The presence of gas phase HNO_3 is somewhat surprising given the fact that the equilibrium vapor pressure is estimated to be significantly smaller than the background pressure in the cryostat chamber of approximately 3×10^{-8} torr. Based on this estimate we expected most of the effusing HNO_3 to "stick" to the cryogenic KCl window and expected therefore a small mass spectrometric signal. NH_3 is a borderline case with a vapor pressure of 10^{-6} torr at 102 *K* and 10^{-7} torr at 96 *K*. FTIR indicates that NH_3 does not condense on the cryostat under the present experimental conditions by itself, even at the lowest temperatures reached. The abundance of HNO_3 in the gas phase is more surprising. Since the heat of condensation and heat capacity of a microns thick film are

insignificant compared to the heat capacity of the KCl substrate, the KCl surface during condensation cannot be more than a few degrees above that of the thermocouple located at the warmest end of the copper substrate holding the KCl window (i.e., farthest from the liquid nitrogen reservoir). Therefore, we judge it likely that the effusing gas is simply partly "missing" the cryogenic surface due to insufficient geometric overlap. Even with the short distance between the exit aperture of the melting capillary and the cryogenic surface (5 cm), a $(\cos)^2$ distribution would have a significant part of the effusing species pass by the 3-cm diameter cryostat assembly.

In order to put the mass spectrometric results into a more quantitative context, a specific mass was followed as a function of probe temperature using identical heating rates and comparable sample sizes. Table I displays the results when the evolution of NH_3 and HNO_3 was followed by monitoring the ion current as a function of temperature.

The characteristic feature of every one of the curves thus obtained is the presence of a single sharp spike indicating a single "explosive" event after which the sample was spent. This explosive decomposition was observed also by monitoring the total pressure (ion gauges) whose readout resulted in a similar sharp spike at the same probe temperature as the mass spectrometric observation. Although the individual ion current vs. temperature curves vary sometimes significantly as to their precise shapes, their characteristic parameters such as onset, width, and maximum agree remarkably well within certain limits. The maximum evolution of both constituents is measured at 182 ± 5°C which is nominally about 10°C higher than the measured melting point at 169.9°C. Under these vacuum conditions, the decomposition of NH_4NO_3 is clearly dominated by the simple dissociation into the acid and base components, as in eq. (1):

$$NH_4NO_3 \Rightarrow NH_3 + HNO_3 \quad (1)$$

The sudden increase in dissociation (an endothermic event) in the absence of any substantial amount of exothermic reaction to drive it very likely results simply from improved heat transfer from the hot capillary walls upon melting of the NH_4NO_3. Based on previous experience with this particular probe design, we expect that a lag in temperature of about 10°C between thermocouple in contact with the bottom of the sample capillary holder and the inside of the capillary itself is not unlikely (see Fig. 2). Consequently,

TABLE I. Temperatures of rapid gas evolution during NH_4NO_3 Decomposition.

Species Monitored	*M/e* Monitored	*T*°C of Maximum Evolution Rate
NH_3	17	187
NH_3	17	190
HNO_3	63	174
HNO_3	63	181
HNO_3	46	182
NH_3	17	185
HNO_3	46	177
		Avg. 182.3

we conclude that the rapid dissociation of NH_4NO_3 under these conditions takes place within a few degrees of (and very probably at) the melting point. In any event, the temperature at which either simple dissociation or exothermic decomposition of NH_4NO_3 take place is not an intrinsic value, but is dependent on the partial pressure of the acid and base species over the condensed phase material.

The current conditions are not those that we expect to yield irreversible decomposition of the acid and base components of NH_4NO_3. Brower and co-workers [3] concluded in a recent study of NH_4NO_3 decomposition that ionic equilibria were important in the lower temperature range, which is of interest here. It was conclusively shown that HNO_3 had a catalytic effect on NH_4NO_3 decomposition, while H_2O and NH_3 inhibited the formation of N_2O and H_2O, the two principal products of NH_4NO_3 decomposition. This finding is consistent with reaction involving self-protonation of HNO_3 in the condensed phase, because the vapor phase does not support ionic reaction mechanisms. Although the extremes of the temperature ranges overlap in the two studies, the conditions are otherwise radically different. In our low pressure study, the evaporation of NH_4NO_3 is so fast that a molten phase with its considerable vapor pressure can not be sustained. Our study therefore addresses predominantly the behavior of the bulk crystalline phase under thermal stress, minimizing secondary bimolecular gas phase reactions and secondary reactions in a liquid or melt phase. The absence of any "real" (irreversible) chemical decomposition of NH_4NO_3 in our case is evidenced by the absence of any N_2O and H_2O, the known products of complete NH_4NO_3 decomposition.

FTIR absorption spectra were obtained by heating NH_4NO_3 to temperatures of about 200°C and collecting the effluent on the cold cryostat window, usually at approximately −190°C. Figure 3 shows a FTIR absorption spectrum of a condensate film that has been collected at −190°C and been allowed to warm up to −50°C. The condensate has been identified as NH_4NO_3 by comparison with a measured absorption spectrum of an ambient temperature authentic polycrystalline sample and by comparison with literature data. By observing the differences in the absorption spectrum upon warming the sample to −50°C, we concluded that a small amount of NH_3, perhaps 10%, was incorporated in the polycrystalline sample of NH_4NO_3. Notably, a characteristic absorption band at 958 cm^{-1} corresponding to the bending mode (umbrella motion) in NH_3, together with other broader absorption bands, disappeared upon warming. Apparently the occluded NH_3 leaves the condensate film in the temperature range −190°C to −50°C. The characteristic bands of NH_4NO_3 are the broad N—H stretch at 3150 cm^{-1}, the asymmetric and symmetric NO_2 stretch at 1440 and 1400 cm^{-1} and the sharp absorption at 825 cm^{-1}. When the identical pyrolysis experiment was performed with the cryostat at ambient temperature, only a very small amount of NH_4NO_3 was observed by FTIR absorption.

The experimental results show that the sublimation of NH_4NO_3 proceeds by way of dissociation of the molten material into its gas phase constituents HNO_3 and NH_3. Subsequently, the gas phase components undergo the acid-base reaction (the reverse of reaction (1)) on the cold surface of the cryostat. In view of the fact that NH_3 does not condense under our conditions, we

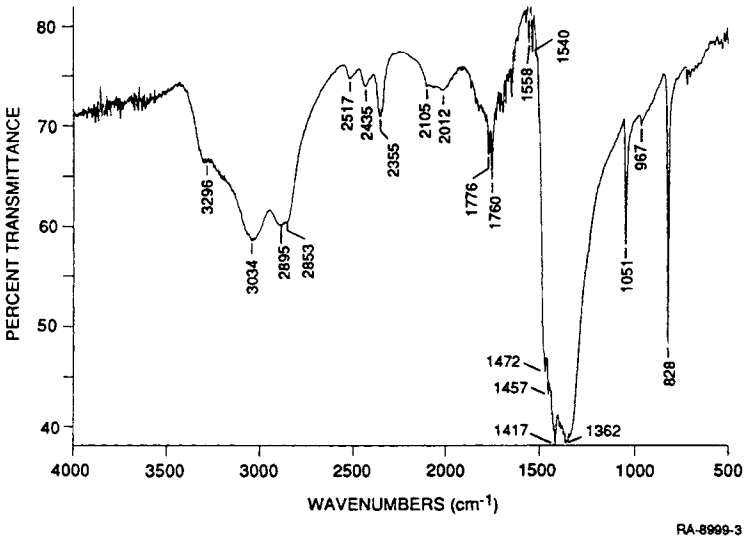

Figure 3. FTIR transmission spectrum after complete evaporation of NH_4NO_3 (probe T = 203°C) after the cryostat has been warmed to −50°C.

suggest that the reformation of NH_4NO_3 proceeds by collisions of gaseous NH_3 with solid HNO_3. The presence of small but significant amounts of NH_3 in condensed films from pyrolysis of NH_4NO_3 is due to a loss of HNO_3, presumably by heterogeneous pathways (see below). We suggest that this loss occurs either on the walls of the capillary sample holder or on some other ambient temperature surface of the vacuum chamber. An important conclusion is the fact that no products of the "real" thermal decomposition of NH_4NO_3, such as N_2O, H_2O, and NH_2NO_2, were found. Therefore, sublimation via simple dissociation seems to be the only important pathway of NH_4NO_3 under the present slow-heating, low-pressure conditions.

NH_2NO_2

In contrast to NH_4NO_3 and ADN, solid nitramide is a deliquescent material and is a molecular crystal whose vapor pressure by far exceeds the background pressure in the vacuum chamber. Therefore, evaporation took place even with the probe at ambient temperature, so that normal pyrolysis experiments, uncomplicated by simple evaporation and thus material loss, were not possible. Nevertheless, decomposition of nitramide is so facile that significant decomposition took place in competition with evaporation. Figure 4 shows a typical mass scan after the introduction of a NH_2NO_2 sample with the cryostat at low temperature and the probe at ambient temperature. Important mass spectral intensities are registered at m/e 17, 18, 28, 30, 44, and lower but significant intensities at 46 and 62. This latter mass corresponds to the molecular ion of NH_2NO_2 and has about 2 to 3% of the intensity of the base peak at m/e 44. The relative intensity of the peaks in the mass spectrum was essentially independent of the temperature of the cryostat, but did change with time (i.e., as the fractional depletion of

the sample in the probe changes). For this reason it is apparent that this mass spectrum does not originate entirely from one single neutral parent species, namely NH_2NO_2. The most noticeable change is in the relative intensity of the fragment masses *m/e* 18 and 44 and the molecular ion, *m/z* 62. As shown below, the former are still observed under conditions where *m/e* 62 has vanished. We conclude therefore, that a condensed-phase or heterogeneous reaction is causing rapid decomposition of NH_2NO_2 according to the following reaction:

$$NH_2NO_2 \Rightarrow N_2O + H_2O \quad (2)$$

We presume that under these rather mild conditions, this reaction occurs according to the accepted base catalyzed mechanism, as recently discussed by Arrowsmith et al. [6]. In any case, in the early stages of the sublimation, Reaction 2 is simply not rapid enough to destroy all of the NH_2NO_2, and some residual intensity is observed at *m/e* 62 indicating the evaporation of NH_2NO_2.

Reaction 2 is exothermic by 26.8 kcal/mol (in the gas phase) if one assumes a sublimation enthalpy of 10.0 kcal/mol for NH_2NO_2 [7–9]. The fact that the observed mass spectrum is independent of the cryostat temperature means that: (a) the heterogeneous decomposition must take place either in the condensed phase or on the walls of the melting tube capillary (probe) or some ambient temperature internal surface of the vacuum vessel, and (b) the partial pressure of the products N_2O + H_2O is not controlled by the cryostat temperature. The cryostat surface represents only a very small fraction of the internal surface area of the vacuum chamber, and the plume of the emanating material from the sampling tube may be partly reaching surfaces other than the cryostat window.

Measurements of ion current at *m/e* 18 (H_2O), 44 (N_2O), and 62 (NH_2NO_2) as a function of probe temperature revealed totally erratic behavior of the ion current with increasing temperature, in that irregular bursts of H_2O and N_2O were monitored using both the mass filter as well as measuring the total pressure (ion gauges). Qualitatively the same erratic behavior was observed for *m/e* 62. This effect was especially pronounced when older samples that had time to undergo thermal decomposition prior to pyrolysis were used. This behavior stands in contrast to the one observed with NH_4NO_3, in that for the latter, the consistent observation was of a single "energetic event" occurring at a reproducible temperature very close to the melting point. Furthermore, with NH_4NO_3, the only ions observable were the acid-base components (i.e., products that are endothermically generated, and which cannot be responsible for autoacceleratory decomposition).

The fact that parts of the bulk sample have already undergone (partial) thermal decomposition at ambient temperature is not surprising in view of the thermal instability of NH_2NO_2. We postulate that small bubbles of NH_2NO_2 decomposition products form throughout the bulk material storing H_2O and N_2O under pressure. While evaporation occurs layer-by-layer, occasionally a "bubble" close to the surface bursts, releasing its content into the gas phase.

Figure 5 displays a FTIR absorption spectrum obtained from an evaporating NH_2NO_2 sample. The effluent was collected at about −190°C (which is

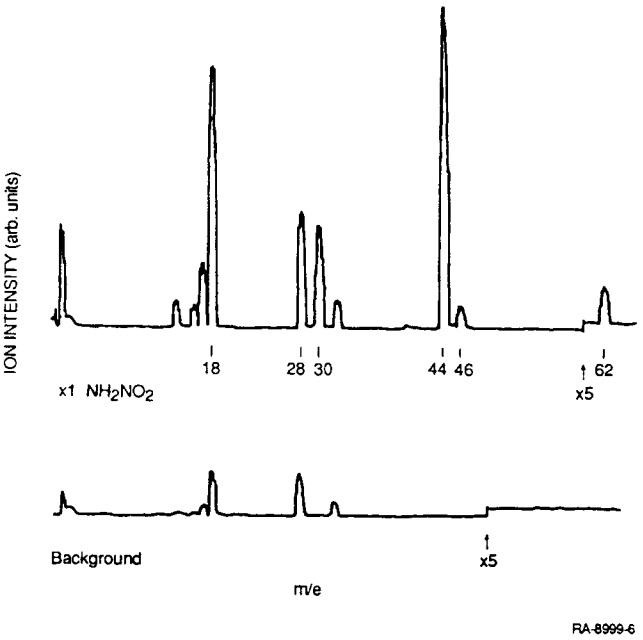

Figure 4. Mass spectrum of material desorbing/decomposing from an ambient temperature probe containing NH_2NO_2, with the cryogenic window held at −180°C.

still too warm for N_2O to condense in view of the low background pressure). Even if major amounts of NH_2NO_2 heterogeneously decomposed according to eq. (2) in the probe, we would still expect a significant IR absorption due to NH_2NO_2 because cryogenic films of amorphous H_2O are relatively weak absorbers. They absorb around 3220 cm^{-1} with shoulders at 3360 and 3150 cm^{-1}. In addition, weaker bands at 2220, 1690, and 800 cm^{-1} can be observed for thick amorphous films of H_2O. The spectrum displayed in Figure 5 is simple and shows the asymmetric and symmetric NH_2 stretch vibrations at 3435 and 3291 cm^{-1} as well as the strong asymmetric and symmetric NO_2 stretch vibrations at 1535, 1491 (doublet), and 1396 cm^{-1}, respectively. The agreement with the literature spectrum obtained by Davies and Jonathan [10] is good, considering that they recorded an absorption spectrum of a crystalline film at ambient temperature, whereas the spectrum of Figure 5 is from a low temperature amorphous thin film. The simplicity and intensity of the spectrum are very suggestive of the existence of relatively isolated units in a disordered solid.

After deposition of the NH_2NO_2 film shown in Figure 5 above was complete, the cryostat was allowed to slowly warm up, and at −113°C large amounts of desorbing H_2O were recorded by mass spectrometry at *m/e* 17 and 18. Upon further warming, the rate of H_2O desorption reached a minimum at −82°C with *m/e* 30, 44, 46, and 62 steadily increasing. Apparently, the large H_2O desorption rate was due to the presence of an amorphous water film deposited in the course of evaporation of NH_2NO_2 from the sample tube and its concurrent heterogeneous decomposition to H_2O via Reaction (2), presumably on the walls of the ambient temperature sample

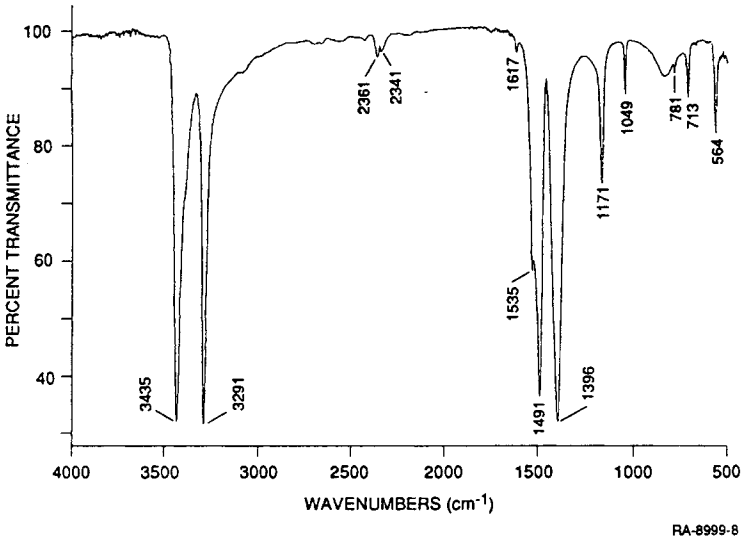

Figure 5. FTIR transmission spectrum of NH_2NO_2 obtained from a thin film deposited onto a −190°C KCl window by evaporation from an ambient temperature probe.

tube. The surge in the masses at *m/e* 30, 44, 46, and 62 stems obviously from evaporation/decomposition of the intact NH_2NO_2 in the cryogenic film. Upon further warming, *m/e* 17, 18, 28, 30, 44, 46, and 62 all increased dramatically to a maximum at −46°C cryostat temperature. From the decrease in the intensity ratios *m/e* 62 ($NH_2NO_2^+$) vs. 46 (NO_2^+) and the intensities at *m/e* 18, 30, and 44 with increasing cryostat temperature in the range −56°C to −38°C (above which *m/e* 62 virtually vanishes), we see that Reaction (2) is facile even at very low temperatures suggesting a heterogeneous pathway. Furthermore, this observation establishes the existence of different parents on the one hand for *m/e* 62, the molecular ion of NH_2NO_2, and on the other hand for some portion of all the other important fragment ions.

In view of a high $\Delta H°$ of 63.5 kcal/mol for dissociation [11] of NH_2NO_2 into NH_2 and NO_2 (assuming a sublimation enthalpy of 10.0 kcal/mol for nitramide) we assume that reaction (2) follows another, heterogeneous route leading directly to N_2O and H_2O. From the recent work of Arrowsmith, et al. [6], and earlier work, [12], we expect that this heterogeneous process is a base-catalyzed reaction. We interpret the occurrence of *m/e* 46 as due to reaction (3), occurring as a minor reaction pathway under the present conditions:

$$(3) \qquad NH_2NO_2 \Rightarrow 0.5N_2O + 0.5HNO_3 + 0.5NH_3$$

In this interpretation, *m/e* 46 is due partly to the evolution of HNO_3, whose base peak is *m/e* 46. Small amounts of NH_3 are obscured due to the abundance of H_2O.

To summarize our observations with NH_2NO_2, under the low-pressure conditions of this experiment, the high vapor pressure of nitramide results in substantial sublimation from the probe, even at ambient temperature, as evidenced by the molecular ion at *m/e* 62, and by redeposition of an

apparently amorphous film of NH_2NO_2 on the cold cryostat, together with some water. Nevertheless, the decomposition pathway to produce N_2O and H_2O (Reaction 2) is so facile that there is substantial decomposition of material evaporated from the cryostat while it is still at −40°C, apparently as a result of catalysis on the chamber walls (which are normally heated to ca. 30°C above room temperature) as well as on the walls of the sample tube. A parallel, but minor, reaction channel leading to HNO_3 is also observed. What stands out is the high rate of both Reactions (2) and (3) at the observed low temperatures.

$NH_4N(NO_2)_2$ (ADN)

Although ADN is, in a formal sense, the dimer of NH_2NO_2, there is no great expectation that ADN will behave substantially like nitramide itself. Reactions (4), (5), and (6) describe several stoichiometric decomposition possibilities:

$$(4) \qquad NH_4N(NO_2)_2 \Rightarrow NH_3 + HN(NO_2)_2 \Rightarrow NH_3 + HNO_3 + N_2O$$

$$(5) \qquad \Rightarrow 2NH_2NO_2 \Rightarrow 2N_2O + 2H_2O$$

$$(6) \qquad \Rightarrow NH_4NO_3 + N_2O$$

This formal relationship of NH_4NO_3 and NH_2NO_2 with ADN is the reason for including the simpler nitrate and nitramide in this study under similar experimental conditions. We will present and discuss the results on ADN in two parts. The first involves pyrolysis experiments of ADN with the cryostat at ambient temperature, at which only the less volatile thermal decomposition products will condense onto the KCl window. The second part involves ADN pyrolysis with a cold cryostat, where only gas phase components not condensing on the cryostat, such as N_2O, NO, and NH_3, are monitored by mass spectrometry. The comparison between these two modes has allowed us to draw some important mechanistic conclusions on the thermal behavior of ADN. In addition, the subsequent evaporation or thermal decomposition of the thin film condensate deposited on the cryostat, leads to some further insights.

ADN Pyrolysis with ambient temperature cryostat. Figure 6a presents a mass scan during the pyrolysis of ADN at 169°C. We observe large mass spectrometric signals at *m/e* 16, 17, 30, 44, and weaker ones at 28 (in addition to the contribution from background air), 46 and 60. We interpret the mass spectrum in terms of evolution of NH_3, NO, and N_2O together with smaller amounts of free $HN(NO_2)_2$ monitored at *m/e* 46 (NO_2^+ and 60 (NNO_2^+). This latter fragment is also observed in electron-impact mass spectra of dimethylnitramine ($(CH_3)_2NNO_2$), a frequently used model compound for explosives studies. Within experimental uncertainty we did not observe the evolution of HNO_3, with the exception of the very first few, lower temperature runs at the beginning of the study, where the vacuum chamber was not warmed to the ca. 60°C used throughout the rest of the study. Under those earlier conditions, *m/e* 46 was more intense than *m/e* 44 (see Figure 6b) and *m/e* 63 was observed as an unambiguous marker for the presence of HNO_3. Figure 6c shows the significant decline of *m/e* 46 that

results from increasing the temperature less than 20°C. In evaluating this result one has to keep in mind that the neutral parent species collides many times with the walls of the stainless steel walls before being ionized (residual gas analysis). The absence of HNO_3 in the later ADN decomposition runs most likely has to do with its heterogeneous decomposition on seasoned metal walls (which were then being heated to about 60°C), a fact alluded to earlier in the discussion of the sublimation of NH_4NO_3. At 170°C, NH_3 and NO evolution increase, whereas *m/e* 46 and 60 decrease substantially. This decrease apparently signals the thermal decomposition of $HN(NO_2)_2$ becoming important at temperatures around 170°C.

When ADN is heated under our conditions, it exhibits "explosive" behavior similar to NH_4NO_3, in that it gives a single pressure burst observed at several masses. The measurement of the time dependent evolution of NH_3 at *m/e* 17, of H_2O at *m/e* 18, and of N_2O at *m/e* 44 as a function of temperature revealed an onset of thermal decomposition of about 90°C and a maximum in decomposition rate at about 155°C. The exact numbers depend somewhat on the heating rate, but the temperature dependent evolution occurs over a significantly narrower temperature range than NH_4NO_3 dissociation (onset at 74°C, maximum rate at 182°C). This difference is thought to have important ramifications in applications of ADN. As with NH_4NO_3 and NH_2NO_2, we observed bursts of H_2O released into the gas phase before the onset of NH_3 release. The importance of this effect again correlates with the quality (purity) and age of the sample. However, our limited set of data does not distinguish between H_2O as a product of a particular decomposition reaction (such as Reaction 2 or 5) or as a result of water-uptake due to the hygroscopic nature of the sample.

Figure 7 presents a FTIR absorption spectrum of the pyrolysate of ADN from a probe heated to 196°C and condensed on an ambient KCl window. We conclude that it corresponds to pure dinitraminic acid ($HN(NO_2)_2$) or "HDN" by virtue of the pyrolysis results discussed below and the simplicity of its IR absorption spectrum. The weak absorption at 3250 cm^{-1} corresponds to the N—H stretching mode. The lineshape of this band suggests an isolated vibrational mode pertaining to a molecular crystal, analogous to the situation encountered in NH_2NO_2. Upon closer examination, the peak positions of HDN (Fig. 7, lower part) do not correspond exactly to those of ADN (Fig. 7, upper part), which indicates that the fundamental frequencies are significantly perturbed in going from HDN to its ammonium salt (ADN). The IR absorption spectrum is characterized by the symmetric and asymmetric NO_2 stretching and bending motions, the latter being split into doublets indicating degenerate interaction of the two NO_2 groups. A more detailed interpretation of the FTIR absorption spectrum lies beyond the scope of this article and will be presented elsewhere [13]. The condensate on the ambient temperature KCl window resulting from the pyrolysis of ADN seems to be pure HDN in view of the identity of the other pyrolysis products, namely N_2O, H_2O, and HN_3 which do not condense under these experimental conditions. Obviously the sticking coefficient of NH_3 onto what is, at least in the bulk, condensed molecular HDN, is too low at ambient temperature to allow regeneration of ADN, in contrast to the case of NH_4NO_3 discussed above, where small amounts of NH_4NO_3 are reformed

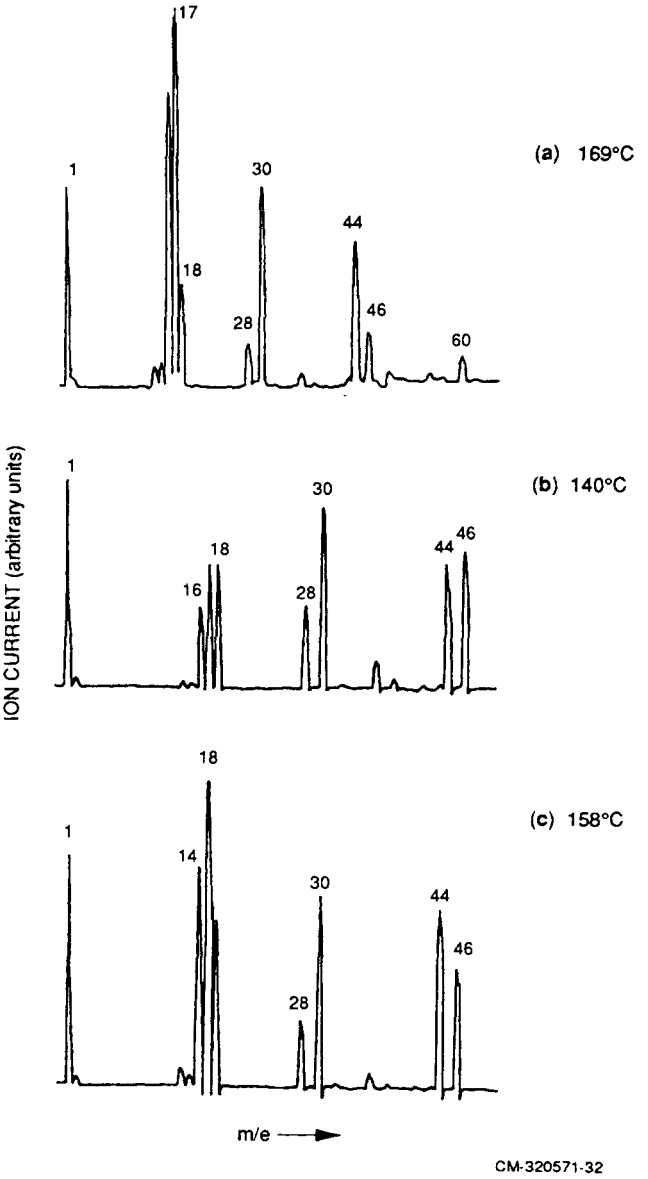

Figure 6. Mass spectra of $NH_4(NO_2)_2$(ADN). (a) 169°C probe temperature and ambient temperature cryostat; (b) 140°C probe temperature taken at beginning of the study; and (c) Same as (b) except probe temperature of 158°C.

at ambient temperature. This is clearly a kinetic effect since ADN is a stable crystalline solid at ambient temperature and the pressures that pertain in this apparatus.

We attempted to regenerate ADN in situ from a deposited film of HDN by exposing the film to various pressures of NH_3 for variable lengths of time at, and slightly above, ambient temperature. The high vacuum system was backfilled with NH_3 at 6×10^{-6} torr for 15 min without measurable

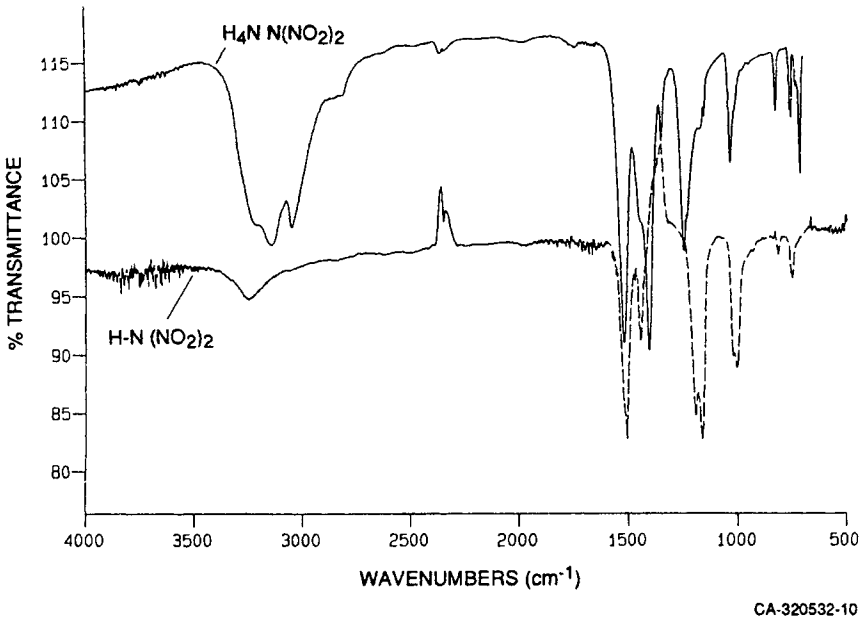

Figure 7. Comparison of FTIR absorption spectrum of $HN(NO_2)_2$ deposited on ambient temperature KCl window from pyrolysis of ADN (probe temperature up to 196°C) with FTIR spectrum of an authentic $NH_4N(NO_2)_2$ sample.

change in the FTIR absorption spectrum. Thus, we did not observe any sign of conversion of the thin HDN film to ADN, whose absorption spectrum will be discussed below. (This NH_3 pressure is substantially higher than the chamber pressure during the course of reformation of ADN on a cold cryostat; it presumably results in at least a NH_3 partial pressure in the immediate vicinity of the cryostat comparable to that which exists during effusion of the ADN components from the pyrolysis probe). This inability to convert HDN to ADN suggests that transport of NH_3 across a thin solid film of ADN is an important limiting factor. Apparently, the regeneration of a solid film of ADN occurs most readily when the components strike the surface together. In analogy to the case discussed above of reformation of ammonium nitrate on the cryogenic window it is thought that NH_3 strikes an adsorbed HDN molecule thereby reforming ADN. By microscopic reversibility, the acid-base dissociation of ADN has to occur sequentially, that is layer-by-layer. However, an obvious exception is the result of "bubble" formation in the interior of the bulk phase at slow heating rates or over long time intervals, as discussed above. For these solid state kinetic phenomena, questions of sample crystallinity and crystal defects are of obvious importance and are not discussed here. An alternative explanation for the inability to regenerate ADN from an already-deposited film of HDN is that the latter film is in reality potassium dinitramide, KDN, formed by ion-exchange on the ambient-temperature cryostat. We consider this less likely because the "HDN" film (Fig. 7) differs significantly in the 700–800 cm^{-1} region from a spectrum of authentic KDN. Furthermore, the authentic

potassium dinitramide is slightly more stable than ADN, whereas the film we have identified here as HDN is less stable than ADN.

The pyrolysis of this thin film of deposited HDN resulted in the rapid evolution of H_2O, NO, and N_2O (all observed by mass spectrometry) immediately after turning on the cryostat heater. Most importantly, no NH_3 was evolved, consistent with our earlier conclusion that ADN pyrolysis yielded pure HDN containing no trapped NH_3 upon condensation. Furthermore, no gas phase HDN was observed (m/e 46, 60) indicating that HDN decomposed on the heated KCl surface before evaporation, in contrast to pyrolysis of ADN in the melting tube capillary at ca. 150°C. The HDN decomposition products detected mass spectrometrically are most likely to arise from areas heated well above 70°C because the heater windings did not wrap around the copper block holding the cryogenic window and whose temperature was measured using a thermocouple wire inserted into the block. The heat transfer from the heater to this copper block was established entirely by heat conduction. We think that a significant fraction of HDN got deposited onto the heater windings in the course of ADN thermal decomposition in the sample tube.

Using the FTIR absorption spectrum as a monitor for the pyrolysis of HDN, we could see that it began to decompose at 70°C and was consumed by 140°C. This result puts an upper limit of ca. 70°C for even short-term stability of condensed phase HDN. However, at ambient temperature (up to 50–60°C) HDN was stable under vacuum for at least 4 h. Interestingly, there was no increase in optical density of HDN (on an ambient-temperature cryostat) upon ADN pyrolysis at probe temperatures in excess of 140°C, even though ADN could be redeposited on a cold cryostat, for probe temperatures approaching 200°C. Apparently, the plume of products emanating from a probe at 140°C or above contains enough decomposition products to promote destruction of any remaining intact vapor phase HDN as it strikes the ambient-temperature cryostat, but not enough to promote decomposition of HDN as it strikes a cold cryostat.

The results presented so far lead to the following conclusions regarding the fate of ADN under thermal stress in vacuum. The pyrolysis of ADN performed in a Pyrex melting tube capillary occurs according to reactions (7), (8), and (9):

$$NH_4N(NO_2)_2 \Rightarrow NH_3 + HN(NO_2)_2 \tag{7}$$

$$HN(NO_2)_2 \Rightarrow N_2O + HNO_3 \tag{8}$$

$$HNO_3 \Rightarrow 0.5H_2O + NO + 0.75O_2 \tag{9}$$

Reaction (7) describes the acid-base dissociation of ADN analogous to NH_4NO_3. Subsequently, HDN partially condenses on the cryostat, while NH_3 is pumped away. The other part of free HDN decomposes on the chamber walls or in the probe according to reactions (8) and (9). We suggest reaction (9) because the dominant feature of HDN decomposition under our experimental conditions seems to be the presence of large amounts of NO observed at m/e 30. In early experiments we obtained unambiguous proof of gas phase HNO_3, whereas in later experiments reaction (9) was apparently much faster than reaction (8), precluding mass spectrometric detection of HNO_3. We believe reaction (9) to be occurring heterogeneously on the walls

of the warmed stainless steel vacuum chamber, as discussed earlier. It is well known [14] that HNO_3 can decompose heterogeneously according to reaction (10).

$$(10) \qquad HNO_3 \Rightarrow NO_2 + 0.5H_2O + 0.25O_2$$

However, if Reaction 10 were occurring here, we should have seen NO_2 as a major reaction product, but it was not observed in significant quantities. On the other hand, we observed large amounts of NO consistent with reaction (9), which we believe is a possible heterogeneous destruction pathway for HNO_3. The exact mechanism of the heterogeneous reactions (9) and (10) is not known. They are both endothermic, by 24.8 and 11.1 kcal/mol, respectively, but are both exoergic at 300°C by 1.8 and 5.3 kcal/mol, respectively [8]. High temperature favors reaction (9) over reaction (10) in view of the significantly higher reaction entropy of 45.9 e.u. (cal/mol-K) vs. 28.4 e.u. A standard thermochemical calculation for pathway (10) reveals that HNO_3 at a total pressure of 10^{-6} torr is more than 99% dissociated at 300 K if the gas-phase products are pumped away, whereas for pathway (9) the degree of decomposition is only 2% under similar conditions. Since this thermochemical estimate [8] does not address the decomposition kinetics, it does not necessarily argue against the large amount of NO released at ambient temperature. It is not known at this time why reaction (10) does not occur under our experimental conditions, especially in view of the more favorable thermochemical parameters of reaction (10) vs. reaction (9). Kinetic constraints on reaction (10) could be responsible, but in the absence of more accurate mechanistic information and measured temperature profiles (that might include hot spots) we will postpone any more quantitative explanations.

The pyrolysis of a thin solid film of HDN on the surface of the KCl substrate occurs according to eq. (11), which is the sum of reaction (8) and (9):

$$(11) \qquad 2HN(NO_2)_2 \Rightarrow 2N_2O + 2NO + H_2O + 1.5O_2$$

We prefer in this case to express the molecular processes using reaction (11) because HNO_3 was not itself observed during decomposition of predeposited HDN films. Presumably, HNO_3 is a reaction intermediate but is not observed due to its rapid decomposition on the walls of the warm vacuum chamber. Another possible decomposition path for HDN is reaction (12), which seems to be endothermic based on the unpublished heat of formation of ADN (−35.6 kcal/mol) [15] and an assumed heat of sublimation of 13.0 kcal/mol. This pathway has the virtue that it explains the presence of NO_2, which is present in small concentrations as ADN is pyrolyzed.

$$(12) \qquad 2HN(NO_2)_2 \longrightarrow H_2O + 5NO + NO_2$$

ADN Pyrolysis with a Cold Cryostat. Essentially identical experiments were performed as described in the previous section with the exception that the cryostat was cooled, usually to between −160°C to −180°C before the start of the pyrolysis experiment. The gas evolution starts with the appearance of NH_3 and N_2O at a probe temperature of 90°C, together with some NO. At 130°C probe temperature, the transmission of the cryogenic

KCl window starts to drop by forming an amorphous H_2O film. NH_3 and N_2O are the dominant species in the mass scans with H_2O starting to appear and a small but significant amount of NO appears. At 150°C, NH_3 and N_2O are still dominant, NO and H_2O are significant and m/e 46 and 60 indicate the presence of gas phase HDN. The surprising occurrence of gas phase H_2O despite a cold cryostat is probably due to the fact that HNO_3 and/or HDN decompose somewhere on the walls of the vacuum chamber (i.e., downstream from the cryostat), releasing NO and H_2O according mainly to reaction (9). At a nominal temperature of about 170°C, NH_3, N_2O, NO, and H_2O are all of comparable magnitude with HDN evolution reaching a maximum. However, the presence of small amounts of HNO_3, which was observed in significant amounts in the early experiments, cannot be excluded. Finally, as 200°C is approached, the maximum rate of evolution of NH_3, H_2O, NO, and N_2O is observed, but by this temperature the HDN flux has decreased significantly. By 220°C, the sample is totally expended, and all signals have fallen to near background levels.

These results are essentially identical to the ones obtained with the ambient cryostat, with the exception perhaps of the abundance of H_2O. Referring to reaction (7) the presence of NH_3 unambiguously points to the dissociation of ADN into its acid and base components. The pronounced abundance of NH_3 in the presence of a cold cryostat is perhaps surprising and is in contrast to the NH_4NO_3 case which shows more modest amounts of NH_3. We take this large amount of NH_3 as an indication of a large extent of decomposition of HDN without which NH_3 is "orphaned" in that it lost its anchor to form ADN on the cold cryostat surface, and/or as an indication of kinetic difficulty in reforming ADN. Consistent with this scenario, we observe the products of the heterogeneous decomposition of HDN, namely N_2O (reaction (8)), and possibly the secondary decomposition products of HNO_3: NO and H_2O (reaction (9)). The small intensity of m/e 46 and 60 at higher temperatures seems to indicate volatile HDN because they are correlated; m/e 46, thus, seems to be the fragment of a condensable component. The present experiments do not address the question of the mechanism by which the heterogeneous decomposition of HDN and HNO_3 occurs. This question can only be addressed by experiments with variable surface-to-volume ratios.

Figure 8 displays a FTIR absorption spectrum of the ADN pyrolysate, where the probe had been heated to $T < 200$°C and the sample collected on the cryostat. A comparison of the absorption spectrum with an authentic polycrystalline sample of ADN dissolved in ethanol and spread over a KCl window revealed that the major component of the condensate was indeed ADN, which had been regenerated from the gas phase components according to the reverse of reaction (7). In comparing the vapor deposited with the polycrystalline ADN (Figs. 8 and 7, respectively), one observes that the intensity of many absorption bands have changed significantly, but the band positions are usually identical within experimental error. A comparison with an ADN sample dispersed in a KBr pellet leads to similar observations. Apparently, ADN is regenerated from its vapor phase components on the cold surface in exactly the same manner as NH_4NO_3. In the microscopic process of ADN regeneration, NH_3 hits an already adsorbed HDN to form

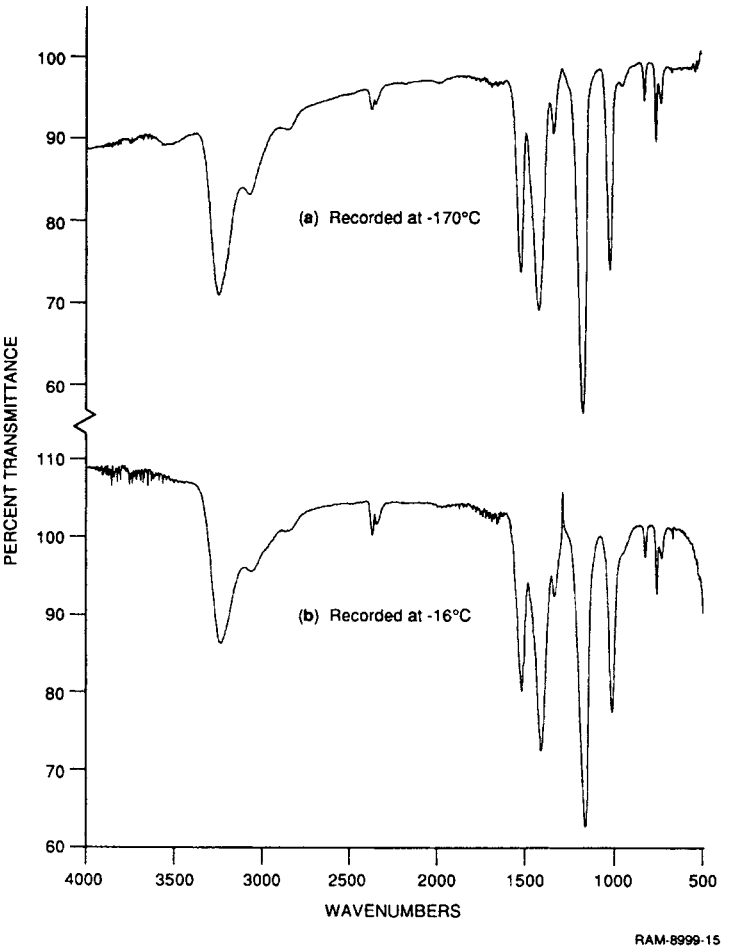

Figure 8. FTIR spectra of ADN decomposition products condensed at −170°C.

the ammonium salt. We have some indications (see below) that the condensed phase also contains some "free" HDN despite the presence of the observed large amounts of NH_3. An investigation of the morphology of the condensed film would be of great interest here because of the differences in the ease of decomposition of ADN and HDN and the consequent implications for storage stability of ADN.

The first increase in IR absorption of the cryogenic KCl window after the start of ADN pyrolysis is caused by the deposition of a pure amorphous H_2O film characterized by a broad peak at 3250 cm^{-1} with two shoulders, as discussed above. At higher pyrolysis temperatures (130°C), a similar broad absorption at 3500 cm^{-1} grows in conjunction with the broad and complex IR absorption at lower frequency due to the presence of the NH_4 ion in regenerated ADN. This higher frequency absorption at 3500 cm^{-1} is also associated with the presence of condensed phase H_2O, as can be seen from mass the spectrometric evidence (see below). From 130° to 200°C probe

temperature, after which the ADN sample is spent, the FTIR absorption spectrum does not change qualitatively except that it grows in intensity.

If the cryostat is subsequently slowly heated up, a H_2O burst is observed at approximately −110°C cryostat temperature without much change in the FTIR spectrum. The H_2O that condensed first on the KCl window giving rise to the amorphous water layer evaporates first, apparently moving through the condensed layer of ADN. The next "wave" of H_2O is released in the temperature range −77° to −61°C and is accompanied by the disappearance of the 3500 cm^{-1} absorption, but otherwise by little change in the FTIR spectrum, as can be seen in the spectrum in Figure 8b. In some cases, when H_2O is desorbed from the film, a sloping baseline appears in the FTIR absorption spectrum, with increasing absorption at higher frequency. Such a change is typical of an increase in surface roughness that increases the scattering properties of the amorphous matrix, and could easily result from the loss of a portion of the matrix.

From about −30°C to ambient cryostat temperature, the only products evaporating are NH_3 and HDN, at a small rate. At the same time, the optical density around 3250 cm^{-1} due to the N—H stretching mode in NH_3 decreases noticeably. This can be described as an annealing process that purifies the ADN layer of those constituents (NH_3 and HDN) that were isolated in the matrix. Concomitantly, the structure of the remaining ADN matrix is annealed, leading to an intensity enhancement of the characteristic ADN absorption. However, we want to point out that HDN condensed on an ambient temperature KCl window is relatively stable at ambient temperature as demonstrated by the persistence of its FTIR absorption spectrum (Fig. 7). With the cryostat returning to ambient temperature, the evolution of NH_3 and N_2O pick up, and beyond that temperature, the pyrolysis products are identical to the case of ADN pyrolysis with ambient temperature cryostat. Concomitantly, the optical density of the KCl window decreases until the original percent transmission is reached at about 200°C.

Summary

The results of ADN pyrolysis show that the behavior of ADN at slow heating rates under high vacuum is controlled by dissociation into its components NH_3 and HDN. On an ambient temperature cryostat, HDN can be trapped and stored indefinitely under high vacuum, whereas it regenerates ADN on a cold cryostat (−190°C) in the presence of gas phase NH_3. This behavior is analogous to the response from NH_4NO_3 in the same type of experiment. The regeneration of ADN must occur by collisions of gas-phase NH_3 onto condensed HDN, similar to the regeneration of NH_4NO_3. In addition, fast secondary (presumably heterogeneous) decomposition of HDN both in the probe as well as on the heated cryostat yields N_2O and HNO_3. The latter secondary pyrolysis product may further undergo fast heterogeneous decomposition in our apparatus, producing mostly NO, which served as a marker for the heterogeneous decomposition of HNO_3. This aspect is also analogous to NH_4NO_3, where an "excess" of NH_3 was observed in thin condensed films of NH_4NO_3 due to HNO_3 decomposition. Decomposition of HDN condensed on the cryostat starts above 70°C, but some gas-phase

HDN generated from ADN survives transit from the heated capillary tube up to 200°C. This behavior may possibly point to a solid-state decomposition mode of HDN.

Pyrolysis of ADN under our experiment conditions does not lead to observation of potential intermediates such as NH_4NO_3 (reaction (6)) or NH_2NO_2 (reaction (5)). Therefore a scission of ADN into its "monomer" NH_2NO_2 does not take place under the present experimental conditions. However, it is possible that the HDN decomposition may bypass HNO_3 entirely to result in NO, N_2O, NO_2, and H_2O.

Acknowledgment

Support of this work by the Energetic Materials Program of the Office of Naval Research, administered by Dr. Richard S. Miller under Contract N00014-90-0115, is gratefully acknowledged.

Bibliography

[1] E. E. Hamel and R. E. Olsen, *U.S. Patent 3,428,667,* Feb. 18, 1969.
[2] J. C. Bottaro and R. J. Schmitt, unpublished work, 1991.
[3] K. R. Brower, J. C. Oxley, and M. Tewari, *J. Phys. Chem.,* **93,** 4029 (1989).
[4] W. A. Rosser, S. Inami, and H. Wise, *J. Phys. Chem.,* **67,** 1753 (1963).
[5] L. Friedman and J. Bigeleisen, *J. Chem. Phys.,* **18(10),** 1325 (1950).
[6] C. H. Arrowsmith, A. Awwal, B. A. Euser, A. J. Kresge, P. P. T. L. Lau, D. P. Onwood, Y. C. Tang, and E. C. Young, *J. Am. Chem. Soc.,* **113,** 172 (1991).
[7] D. D. Wagman, W. H. Evans, V. B. Parker, R. H. Schumm, I. Halow, S. M. Baily, K. L. Churney, R. L. Nuttall, *J. Phys. Chem. Ref. Data,* **11,** Suppl. 2, (1982).
[8] D. R. Stull and H. Prophet, *JANAF Thermochemical Tables,* National Standard Reference Data Series, NSRDS-NBS37, Nat. Bur. Stand., Washington DC, 1971.
[9] D. F. McMillen and D. M. Golden, *Ann. Rev. Phys. Chem.,* **33,** 497 (1982).
[10] M. Davies and N. Jonathan, *Trans. Farad. Soc.,* **54,** 469 (1958).
[11] J. O. Ray and R. A. Ogg, Jr., *J. Phys. Chem.,* **60,** 1956 (1956).
[12] J. N. Bronsted and K. Pedersen, *Z. Phys. Chem.,* **108,** 185 (1924).
[13] M. J. Rossi, in preparation, 1993.
[14] S. Svensson and E. Ljungstroem, *Int. J. Chem. Kinet.,* **20,** 857 (1988).
[15] R. Schmitt, private communication, August 1992, SRI International.

Received October 28, 1992
Accepted February 11, 1993